ORTHO-POSITRONIUM DETECTION WITH A HIGH-RESOLUTION PET SCANNER*

Firas Abouzahr, John P. Cesar, Michael Gajda, Alex S. Kuo
Karol Lang, Jingchun Liu, Aryan Ojha, Marek Proga

Department of Physics, University of Texas at Austin, Austin, TX 78712, USA

Paulo Crespo, Andrey Morozov

Laboratório de Instrumentação e Física Experimental de Partículas
3004-516 Coimbra, Portugal

Received 30 July 2024, accepted 12 October 2024, published online 27 November 2024

We have designed and fabricated a research brain time-of-flight PET scanner for *in vivo* range verification for the proton therapy. Featuring state-of-the-art spatial, timing, and energy resolutions, this scanner can also serve as a precision tool for positronium imaging. We present initial studies using our scanner to search for ortho-positronium (o-Ps) 3γ self-annihilation events within the plastic casing of a Na-22 button source. By detecting triple coincidences and filtering out false events, such as those produced by the Compton scattering of back-to-back 511 keV gammas, we have successfully observed the signature of true o-Ps formation. This was achieved through four filtering techniques based on energy, decay plane orientation, time-of-flight, and momentum. The experimental results are guided by Geant4 simulations. Additionally, a control study was conducted using a metal-encased Ge-68 line source, demonstrating the expected quenching of o-Ps $\rightarrow 3\gamma$ events in metals compared to plastics.

DOI:10.5506/APhysPolBSupp.17.7-A1

1. Introduction

Positronium is the bound state formed between an electron and a positron. In its ground state, positronium can be found as a spin-1 triplet state, ortho-positronium (o-Ps), or as a spin-0 singlet state, para-positronium (p-Ps). Charge conjugation symmetry in electromagnetic interactions demands o-Ps self-annihilate into an odd number of photons, excluding $n = 1$, with $n = 3$ occurring with the highest likelihood, and p-Ps

* Presented at the 5th Jagiellonian Symposium on *Advances in Particle Physics and Medicine*, Cracow, Poland, June 29–July 7, 2024.

into an even number with $n = 2$ occurring with the highest likelihood. The lifetimes and decay schemes of ortho- and para-positronium in vacuum are well predicted by non-relativistic quantum electrodynamics (nrQED) [1, 2]. For this reason, positronium has been widely used for precision tests of the Standard Model as well as new physics searches [3–5].

In practice, positronium lifetimes and decay probabilities depend on the environment in which it is formed. For example, while the o-Ps is formed in about 30% of electron–positron interactions, in most materials o-Ps $\rightarrow 3\gamma$ decays make up roughly only 0.5% of events due to the dominance of pick-off, the process by which the positron directly annihilates with an electron in the surrounding environment rather than self-annihilating with its bound electron [2]. The 3γ fraction ($f_{3\gamma}$), the ratio between the number of total 3γ events and back-to-back 511 keV gamma events, is higher in porous materials, where the o-Ps can form in vacancies of low electron density to avoid pick-off [2, 6]. In recent years, the use of positronium formation in positron emission tomography (PET) has become of great experimental and clinical interest for positronium lifetime imaging for *in vivo* tissue assessment, and is one of the driving motivations for this study [7–11].

The Time-of-Flight PET for Proton Therapy (TPPT) consortium has designed and fabricated a high-resolution, time-of-flight PET scanner optimized to provide in-beam range verification for proton therapy (Fig. 1) [12–15]. The scanner's modular technology consists of 8×8 LYSO scintillator arrays, coupled one-to-one with Hamamatsu S14161-3050HS-08 silicon photomultiplers (SiPMs) [16]. The readout and data acquisition electronics are provided by TPPT collaborators, PETsys Electronics [17]. Preliminary results illustrate that the TPPT scanner has a coincidence time resolution (CTR) of about 230 ps, which can be reduced to 180 ps by selecting the

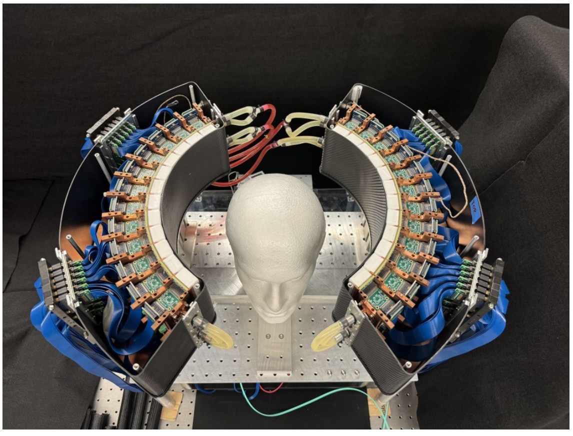

Fig. 1. The commissioned TPPT scanner with its electronics exposed.

highest-performing channel pairs, an average energy resolution of 6.4% at 511 keV, and a spatial resolution of about 2 mm [15, 18, 19]. In this study, we test the feasibility of using the TPPT scanner for positronium imaging by using it to observe the low branching fraction decay o-Ps $\rightarrow 3\gamma$.

2. Methods

2.1. Experimental setup

A 4.5 μCi button source was placed at the isocenter of the TPPT scanner, located 162.5 mm from each detector face. At this distance, the azimuthal and polar angular separation between pixels is 1.13°. The button source has a small volume of Na-22 in the center encased in PMMA plastic with a diameter of 26 mm and a height of 3.2 mm. The plastic casing around the source acts as the medium for positronium formation. Triple coincidence data was acquired with this source for 30 minutes to search for o-Ps 3γ decays.

2.2. Monte Carlo simulations

Analysis of experimental data is guided by the Geant4 Monte Carlo simulations [20]. The simulations incorporate the full TPPT detector geometry with a point source placed in the isocenter. The simulations allow for the specification of $f_{3\gamma}$ and each event, double or triple, is followed by a 1274 keV prompt gamma to replicate the decay scheme of Na-22. The physics model handling the energy and angular distributions for 3γ decays in simulation is based on the theorems described by Kamińska *et al.* [21] and was originally implemented in GATE by Bała [21–23]. For this study, we set $f_{3\gamma} = 0.5\%$. The simulated single-photon energy spectrum for 3γ events agrees well with the accepted spectrum predicted by nrQED (Fig. 2) [1]. The positron range and positronium lifetimes are not yet considered in simulation.

2.3. False triple coincidences

Positive identification of true o-Ps self-annihilation events requires the ability to filter out false triple coincidences. The first, and most prominent, source of false coincidences stems from back-to-back gammas, where one of the gammas Compton scatters and re-interacts in a different detector channel. The second false coincidence stems from a prompt gamma contributing as the third signal in the coincidence. The third type of false event is random coincidences, where gammas from independent events are accidentally grouped together in time. These false triple coincidences are visualized in Fig. 3.

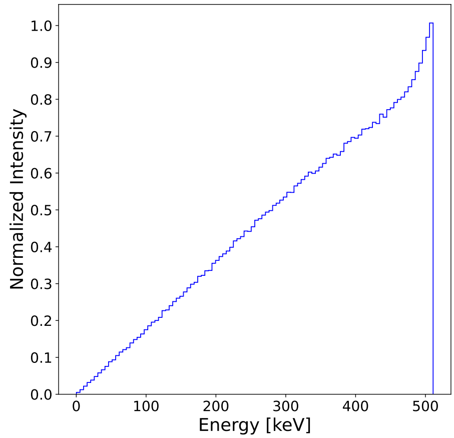

Fig. 2. Simulated single-photon energy spectrum for 3γ decays.

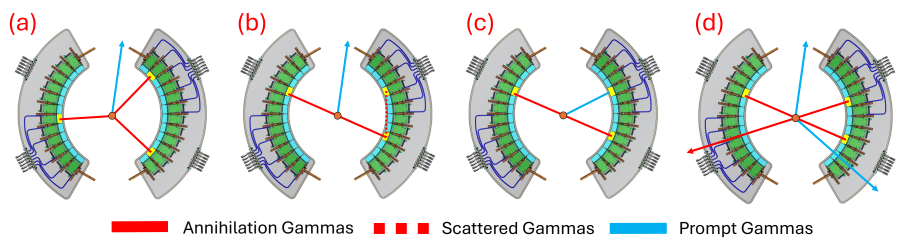

Fig. 3. Visualization of different triple coincidences observed in the TPPT detector: (a) True 3γ coincidence, (b) Back-to-back gammas with Compton scattering, (c) Two gammas from an annihilation event with the third signal coming from a prompt gamma, and (d) Random coincidence, the example shown displays two independent back-to-back gamma events. The yellow blocks represent scintillation events.

2.4. Background filtering techniques

We employ four background filtering techniques based on energy, decay plane orientation, momentum, and time-of-flight to remove false coincidences and isolate true o-Ps $\rightarrow 3\gamma$ events. These filtering techniques are, in part, inspired by the pioneering work of the J-PET Collaboration [24, 25]. Two distinct energy cuts are imposed on the data. First, we only retain events falling at least 1.5σ below the Gaussian fit to the 511 keV photopeak. This helps reject contributions from the known back-to-back gammas as well as high-energy prompt gamma depositions. Varying the cut from 1σ to 2.5σ changed the sample size by only 10%, so 1.5σ was chosen to try to optimize the removal of 511 keV photoelectric absorptions without cutting an excess of 3γ depositions. The second energy cut requires that the energy of the three signals must sum to 1022 ± 100 keV. The 200 keV window was selected to account for energy resolution as well as to accept 3γ events with the Compton scattering. Shrinking or expanding the window by 50 keV did not make statistically significant changes to our final results. A decay plane cut was imposed by ensuring that the plane formed between the three signals pass within ± 1.5 mm of the isocenter. Momenta are used to isolate true 3γ events. Defining the angles between reconstructed momentum vectors as $\theta_{12} < \theta_{23} < \theta_{13}$, the relation $\theta_{23} - \theta_{12}$ *versus* $\theta_{12} + \theta_{23}$ can be used to identify the origin of triple coincidences. Figure 4 plots this angular correlation using the truth momenta of simulated 3γ events. The events all fall within a well-defined triangle with its right angle at $\theta_{12} + \theta_{23} = 180°$, which follows from conservation of momenta, and agrees well with other studies [2, 24].

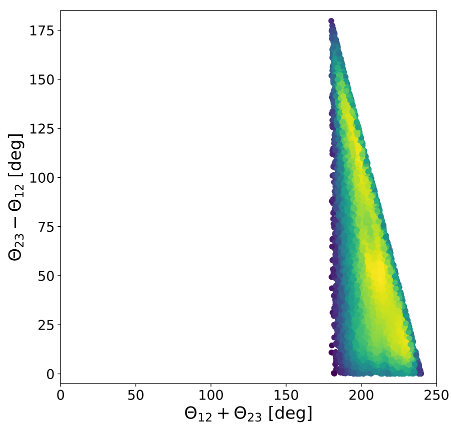

Fig. 4. Incident angular correlations of simulated 3γ decays.

3. Results

3.1. Simulation results

Figure 5 illustrates the angular correlations between reconstructed momentum vectors in simulation for only back-to-back gamma events (a), back-to-back events each followed by a prompt gamma (b), only true 3γ events (c), and true 3γ events each followed by a prompt gamma (d). The back-to-back gammas form a clear line at $\theta_{12} + \theta_{23} = 180°$, which follows from one of the two back-to-back gammas Compton scattering and contributing the third deposition in the coincidence. When we simulate back-to-back gammas with each event followed by a prompt gamma (Fig. 5 (b)), there is a clear formation of a line slopping from $\theta_{12} + \theta_{23} = 180°$ down to $0°$.

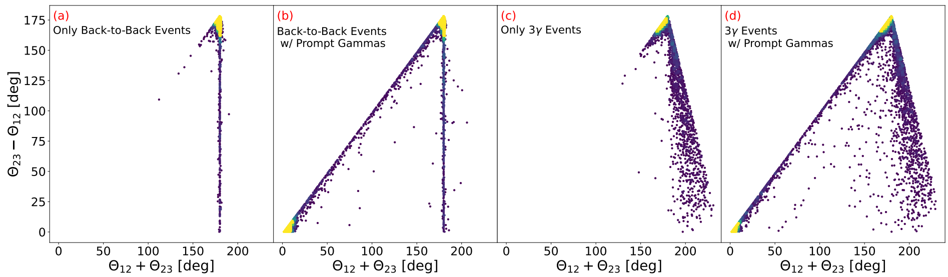

Fig. 5. Angular correlation plots from reconstructed momenta in simulation for (a) Only back-to-back 511 kev gamma events, (b) Back-to-back gammas each followed by a prompt gamma, (c) Only 3γ events, and (d) 3γ events each followed by a prompt gamma.

With only true 3γ events simulated (Fig. 5 (c)), the events fall within the expected right triangle as predicted from Fig. 4. However, there are some important features in this distribution that should be noted. First, there is an aggregation of events sloping from $\theta_{12} + \theta_{23} = 180°$ down to about 150°. This stems from events where only two of the three gammas interact in the detector and one Compton scatters to contribute the third signal. Second, compared to Fig. 4, there is a lack of events in the bottom right corner of the triangle which arises from the detector not being a full ring geometry.

3.2. Experimental results

Figure 6 (a) shows the angular correlation from experimental data with both energy and decay plane cuts imposed. This result agrees well with the angular correlations from simulations with $f_{3\gamma} = 0.5\%$ (Fig. 6 (b)). In the experimental data, there is a broadening effect of the back-to-back gamma line at $\theta_{12} + \theta_{23} = 180°$. Experimentally, the momentum of each gamma is reconstructed with the assumption that it interacted in the middle of the crystal leading to imprecise reconstruction compared to simulation which uses the true position. Moreover, in these preliminary studies, positron range is not considered, which could also contribute to this dispersion effect. Based on this broad line centered at 180°, we take events at $\theta_{12} + \theta_{23} \geq 186°$ to be potential true o-Ps $\rightarrow 3\gamma$ events. The larger spread of events across the experimental data compared to simulation can be attributed to random coincidences, which are not yet accounted for in simulation. After energy filtering, simulations show that 97.1% of events with $\theta_{12} + \theta_{23} \geq 186°$ are true 3γ decays. However, random coincidences could significantly reduce this percentage in experimental data.

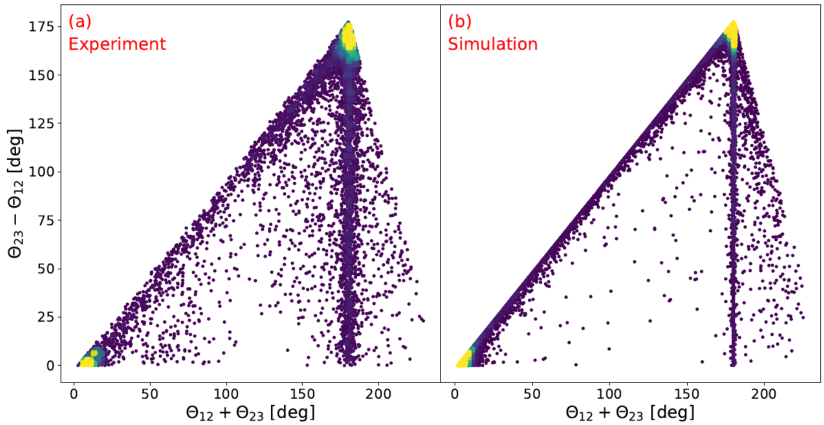

Fig. 6. (a) Angular correlation from the experimental data with energy and decay plane cuts. (b) Angular correlation from simulation with $f_{3\gamma} = 0.5\%$.

Time-of-flight information can be used to reject random coincidences and better gauge the number of true 3γ events. Figure 7 plots the number of potential o-Ps $\rightarrow 3\gamma$ events within the $\theta_{12} + \theta_{23} \geq 186°$ region as a function of an imposed detection time difference requirement across all three signals ($\Delta t_{12}, \Delta t_{23}, \Delta t_{13}$). As the time windows are made more stringent, the number of true o-Ps $\rightarrow 3\gamma$ candidate events decreases. The proper time window to reject as many random coincidences as possible, while optimizing the retention of true 3γ events, will be guided by simulation in the future.

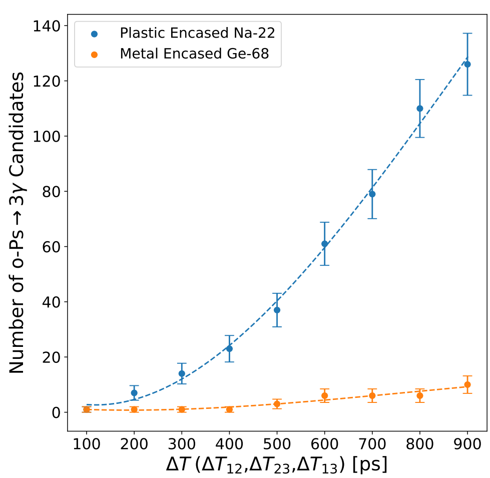

Fig. 7. Number of o-Ps candidates *versus* detection time differences across all three signals.

In the same figure, the orange data shows the results from a control study — experimental data acquired with the TPPT detector using a Ge-68 line source encased in stainless steel metal with all the same processing and background filtering techniques applied to it. Both datasets are fit with cubic polynomials to better illustrate their trends. The error bars are from the Poisson counting uncertainty, $\sqrt{N}$. Due to the high electron density and low porosity of metals, o-Ps $\rightarrow 3\gamma$ events are expected to be quenched compared to those in most plastics [26–28]. The control data indeed illustrates this 3γ quenching effect in the metal-encased Ge-68 source, further validating that we observed true o-Ps self-annihilations in the plastic of the Na-22 source.

4. Conclusion

We have observed strong evidence of o-Ps $\rightarrow 3\gamma$ decays from positronium formation within the PMMA plastic case of a Na-22 button source using the TPPT PET scanner. The results were guided by Geant4 simulations and follow from background filtering techniques based on energy, decay plane, momentum, and timing to remove false coincidences and isolate true 3γ events. Finally, the observed quenching of 3γ events in a Ge-68 source encapsulated in stainless steel helps validate that true o-Ps self-annihilations were observed with the plastic-encased Na-22 source.

The TPPT project has been made possible by a grant from the UT-Portugal program at the University of Texas at Austin. We appreciate the informative discussions with Paweł Moskal and Wiktor Mryka from the J-PET Collaboration. We would also like to thank the organizers of the 5$^{\mathrm{th}}$Jagiellonian Symposium on *Advances in Particle Physics and Medicine*, Paweł Moskal and Ewa Stępień, for their hospitality during the conference.

REFERENCES

[1] A. Ore, J.L. Powell, *Phys. Rev.* **75**, 1696 (1949).
[2] P. Moskal *et al.*, *Phys. Med. Biol.* **64**, 055017 (2019).
[3] A. Rubbia, *Int. J. Mod. Phys. A* **19**, 3961 (2004).
[4] P.A. Vetter, S.J. Freedman, *Phys. Rev. Lett.* **91**, 263401 (2003).
[5] P. Moskal *et al.*, *Nat. Commun.* **15**, 78 (2024).
[6] M.D. Harpen, *Med. Phys.* **31**, 57 (2003).
[7] J. Qi, B. Huang, *IEEE Trans. Med. Imag.* **41**, 2848 (2022).
[8] P. Moskal, E.Ł. Stępień, *Bio-Algorithms Med-Systems* **17**, 311 (2022).
[9] P. Moskal *et al.*, *Sci. Adv.* **10**, eadp2840 (2024).

[10] P. Moskal *et al.*, *Sci. Adv.* **7**, eabh4394 (2021).

[11] P. Moskal, in: «Proceedings of 2019 IEEE Nuclear Science Symposium and Medical Imaging Conference (NSS/MIC)», Manchester, UK, 2019, pp. 1–3.

[12] «TOF-PET for Proton Therapy (TPPT) — In-beam Time-of-Flight (TOF) Positron Emission Tomography (PET)», consortium of the University of Texas at Austin (K. Lang, PI), UT M.D. Anderson Cancer Center (M. Sahoo, PI), `https://utaustinportugal.org/projects/tppt/`

[13] F. Abouzahr *et al.*, *Phys. Med. Biol.* **68**, 125001 (2023).

[14] F. Abouzahr *et al.*, *Phys. Med. Biol.* **68**, 235004 (2023).

[15] K. Klein *et al.*, poster presentation at the 12$^{\rm th}$ International Conference on Position Sensitive Detectors, University of Birmingham, United Kingdom, 12–17 September, 2021.

[16] «Hamamatsu silicon photo-multipliers», Hamamatsu Photonics, Hamamatsu City, Japan.

[17] PETSys Electronics S.A., Taguspark, Ed. Tecnologia I, 24 and 26, 2740-257, Portugal.

[18] K. Lang, *Bio-Algorithms Med-Systems* **18**, 96 (2022).

[19] J. Cesar *et al.*, poster presentation at the 2022 IEEE Nuclear Science Symposium, Medical Imaging Conference and Room Temperature Semiconductor Detector Conference, Milano, Italy, 05–12 November, 2022.

[20] Geant4 Collaboration (S. Agostinelli *et al.*), *Nucl. Instrum. Methods Phys. Res. A* **506**, 250 (2003).

[21] D. Kamińska *et al.*, *Eur. Phys. J. C* **76**, 445 (2016).

[22] S. Jan *et al.*, *Phys. Med. Biol.* **49**, 4543 (2004).

[23] D. Sarrut *et al.*, *Phys. Med. Biol.* **66**, 10TR03 (2021).

[24] K. Dulski *et al.*, *Nucl. Instrum. Methods Phys. Res. A* **1008**, 165452 (2021).

[25] P. Moskal *et al.*, *Acta Phys. Pol. B* **47**, 509 (2016).

[26] R. Lagu, V. Kulkarni, B. Thosar, G. Chandra, *Proc. Indian Acad. Sci.* **69**, 48 (1969).

[27] R.M. Singru, in: C.N.R. Rao (Ed.) «Modern Aspects of Solid State Chemistry», *Springer*, Boston, MA 1970, pp. 329–342.

[28] S.D. Bass, S. Mariazzi, P. Moskal, E. Stępień, *Rev. Mod. Phys.* **95**, 021002 (2023).